NEW TIME-DISTANCE HELIOSEISMOLOGY RESULTS FROM THE SOI/MDI EXPERIMENT

T.L. DUVALL, JR.
Laboratory for Astronomy and Solar Physics, NASA Goddard Space Flight Center, Greenbelt, MD 20771, USA

AND

A.G. KOSOVICHEV AND P.H. SCHERRER
W.W. Hansen Experimental Physics Laboratory, Stanford University, Stanford, CA 94305, USA

Abstract. The SOI/MDI experiment on SOHO has some unique capabilities for time-distance helioseismology. The great stability of the images observed without benefit of an intervening atmosphere is quite striking. It has made it possible for us to detect the time of flight for separations of points as small as 2.4 Mm in the high-resolution mode of MDI (0.6 arcsec/pixel). This has enabled us to detect the supergranulation flow beneath the surface. Using a tomographic inversion technique, we can now study the 3-dimensional evolution of the flows near the solar surface.

1. Introduction

In time-distance helioseismology, the time-of-flight of acoustic waves is measured between various points on the solar surface. In the geometrical acoustics approximation, the waves can be considered to follow ray paths that depend only on a mean solar model, with the curvature of the ray paths being caused by the increasing sound speed with depth below the surface. The time-of-flight is affected by various inhomogeneities along the ray path, including flows, temperature inhomogeneities, and magnetic fields. By measuring a large number of times between different locations and using an inversion method, it is possible to construct 3-dimensional maps of the subsurface inhomogeneities.

Figure 1. The reciprocal ray paths between two surface points, x_1 and x_2. The difference between the reciprocal travel times, $\tau_+ - \tau_-$, is primarily determined by the flow velocity along the ray path, while the mean, $\frac{1}{2}(\tau_+ + \tau_)$ is sensitive to the sound speed and to the second-order effects of the flow.

lead to the very distinctive signature of the travel time being different for the opposite direction of travel between the same points. We have found no other effect which can yield this signature.

A magnetic field in the region of wave travel can also lead to travel time anisotropy (Duvall *et al.* 1996*a*). This is somewhat harder to isolate, as the distinctive signature of the field is that waves travelling along the field direction have a different wave speed than waves travelling perpendicular to the field. For some field geometries, it is possible to set up pairs of rays that intersect at right angles to look for this type of signature, but it is more difficult as the two rays have different paths except at the location where they intersect, and so other inhomogeneities can confuse the issue. The general form of rays below the surface is shown in Fig. 2. In this paper the effect of magnetic anisotropy is not considered.

3. Observations

For this study we have used 8.5 hours of Doppler images from January 27, 1996 taken in the high resolution mode of MDI, which has 0.6 arcsec/pixel. To study convection near the surface, it is necessary to use fairly short intervals in order that the evolution not be too great during the observing

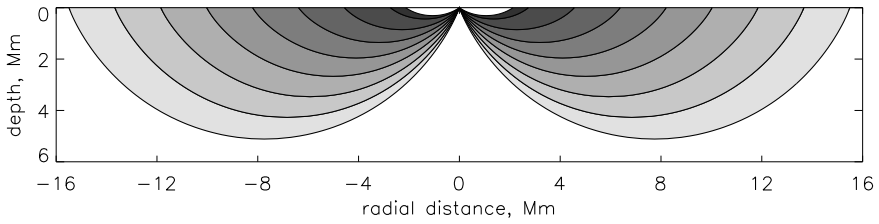

Figure 2. The rays going from the center to the different annuli. The ray paths are curved because of the increasing sound speed with depth. The sound speed increases from 7 km/s near the surface to 23 km/s at 5 Mm depth. The horizontal separation between surface points is approximately π times the depth. The measured travel times are sensitive to the component of velocity along the particular ray path.

interval. On the other hand, it is necessary to observe for some length of time in order to get a statistical sample of waves. The 8.5 hours is a compromise between these two competing requirements, with the supergranule lifetime of about 1 day putting an upper limit on how long to observe. Another point is that we need to observe for longer than the travel time as the correlation that we are detecting arises from the same wave travelling from one location to the other through the subsurface layers. The travel times used in the present study are for surface point separations in the range 6-30 Mm, and are in the interval 17-34 minutes.

4. Analysis

To get the travel times between different locations, we calculate the temporal cross correlation function between the data at one location and the data within an annulus at some great-circle distance from the point. We look at both positive and negative lags of the correlation function, as this can tell us in which direction the waves are travelling. For example, a signal at location 1 first and at location 2 later will lead to a signal at one sign of lag while a signal at location 2 first will lead to a correlation at the opposite sign of lag.

The cross correlation function, averaged over a number of origins, is shown in Figure 3, along with a curve showing the time versus distance for a simple theory. If we imagine generating a pulse of acoustic energy at the surface that propagates along the ray paths to the distant location, we might expect to see a pulse at the distant location. But in fact we see something that is much broader and really looks like a wave packet with a period of five minutes, and a width in time of about 1/bandwidth of our oscillation power spectrum, or $(1\ \mathrm{mHz})^{-1}$=17 min. This makes sense, because

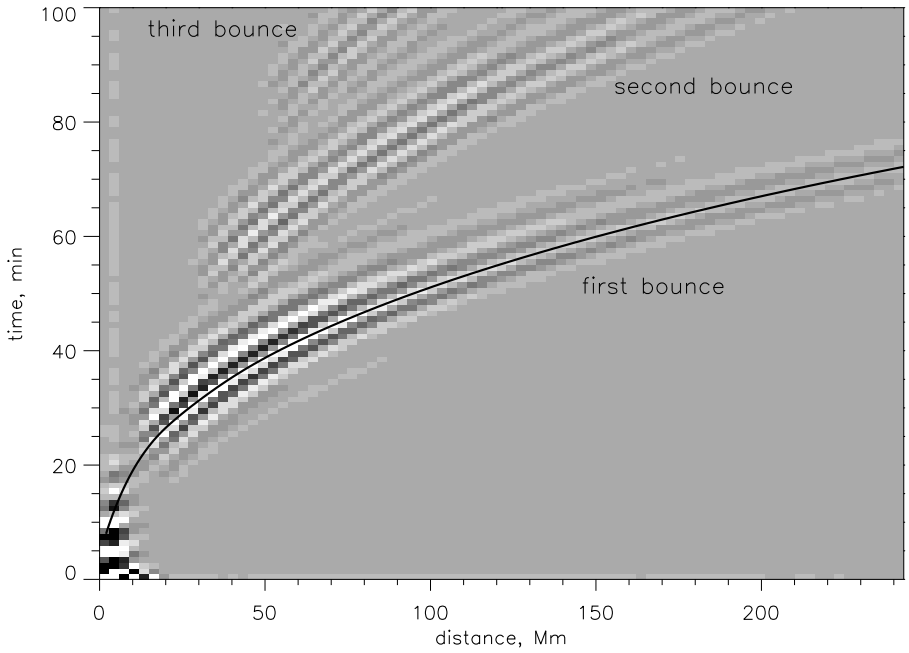

Figure 3. A mean cross covariance function for the data. The solid line is a theoretical plot of the time for waves to travel along a ray path for the specified great-circle distance. The grayscale picture is the cross covariance function. The first, second and third bounces are visible near 30 min., 60 min., and 90 min. The fine structure in each of the ridges is caused by the finite bandpass of the oscillations.

the pulse that we generated at the surface had an infinite bandwidth and so could make a zero-width feature in the correlation function. As shown earlier by Duvall *et al.* (1993), the correlation function that we observe is the Fourier transform of the power spectrum. The remaining features in Figure 3 correspond to the multiple bounces. If there is a correlation observed at time t and at distance d, there will be a similar signal at $n \times t$ and $n \times d$, where n is integral.

In some earlier work (Duvall *et al.* 1993), the correlation function was rectified by using the analytic signal formalism, and times were measured from this signal which is the envelope of the correlation function. Later it was found that the higher frequency structure in the correlation function actually is a more sensitive measure of subsurface inhomogeneities (Duvall *et al.* 1996*a*). In that work, the location of one of the fine structure peaks was determined by measuring the zero crossing of the instantaneous phase of the correlation function. For the present work, this has been further refined (Kosovichev and Duvall 1996). A 20-minute interval in the neighborhood of

the peak in the correlation function is fit to a Gaussian wave packet, with independent parameters for the location of the envelope, the location of one of the fine structure peaks, the amplitude and width of the Gaussian, and the frequency. All the results shown are from the location of the fine structure peak.

Following Duvall *et al.*(1996*a*), we compute the mean cross correlation for waves travelling both out from the center to the annuli and the reverse. The difference of the times measured from these cross correlations is a measure of divergence of the flow. It could be due to either a downflow near the central location or to an average horizontal outflow (or inflow) near the annulus. In addition to this divergence signal, a mean time is computed for the inward and outward waves. To get more directional information about flows, we break up the annulus surrounding a point into quadrants, centered on the four directions north, south, east, west (Duvall *et al.* 1996*b*). We then average the cross correlations for eastward and westward waves separately. The travel times are measured separately for the eastward and westward waves by the above procedure. To get a signal proportional to a flow, we then take the difference of these two times. The same procedure is applied to north-south propagation.

5. Inversions

The images are used in a ray-theory inversion (Kosovichev 1996, Kosovichev and Duvall 1996). The region of the Sun is separated into a 3-D grid of inhomogeneities with the same horizontal sampling interval as the input images (4.3 Mm) and an equal increment in depth covering the same depth range as the input data. The number of grid points in depth is taken to be the same as the number of input images, and, in this case, is 8. Each grid point has four independent variables, the three components of flow velocity and a sound speed inhomogeneity. No attempt is made to satisfy any conservation equations, like the continuity equation.

In Figure 4, we show the inversion results for the subsurface layer. The flow field mainly consists of isolated outflows of the characteristic size of 30 Mm, corresponding to supergranules observed on the surface. One advantage of studying near-surface regions is that we do have extra information at the surface that we would not have for the deep interior. In Figure 5 we show a vertical cut showing the subsurface flows. It would appear that the pattern of horizontal motions at the surface only persists to a few Megameters in depth. But it is probably premature to draw strong conclusions yet because of the newness of the method.

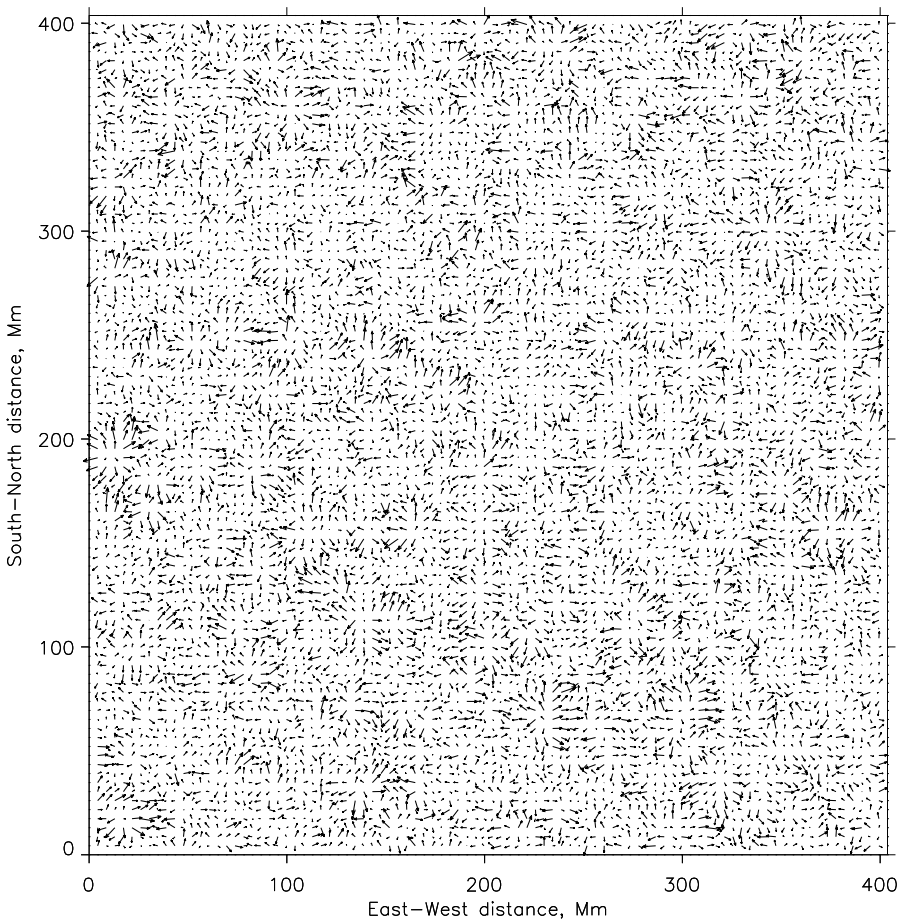

Figure 4. The horizontal flows near the surface from the inversion procedure are shown as vectors.

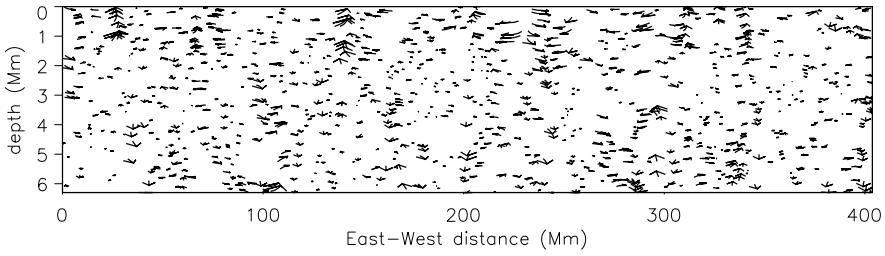

Figure 5. A vertical cut showing the component of flow in the plane. The flow is again shown as vectors.

Conclusions

We have shown that there is detailed information about the subsurface inhomogeneities contained in the helioseismology data. We have also shown it should be possible to extract this information and have shown some first-order attempts to do so. We would appear to have an exciting new window into the solar interior.

Acknowledgments

The authors acknowledge many years of effort by the engineering and support staff of the MDI development team at the Lockheed Palo Alto Research Laboratory (now Lockheed-Martin Advanced Technology Center) and the SOI development team at Stanford University. SOHO is a project of international cooperation between ESA and NASA. This research is supported by the SOI-MDI NASA contract NAG5-3077 at Stanford University.

References

D'Silva, S., 1996, *Astrophys. J.*, 469, 964.

D'Silva, S., Duvall, T.L.Jr., Jefferies, S.M. & Harvey, J.W., *Astrophys. J.*, 471, 1030.

Duvall, T.L.Jr., Jefferies, S.M., Harvey, J.W., & Pomerantz, M.A., 1993, *Nature*, 362, 430.

Duvall, T.L.Jr., D'Silva, S., Jefferies, S.M., Harvey, J.W., & Schou, J., 1996*a*, *Nature*, 379, 235.

Duvall, T.L.Jr., Kosovichev, A.G., Scherrer, P.H., & Milford, P.N., 1996*b*, *BAAS*, 188, 49.08

Kosovichev, A.G., 1996, *Astrophys. J.*, 461, L55.

Kosovichev, A.G. & Duvall, T.L.Jr., 1997, in: "Solar Convection and Oscillations and their Relationship", eds J. Christensen-Dalsgaard, F. Pijpers & C.S. Rosenthal, Proc. of SCORe'96 Workshop, Aarhus (Denmark), May 27-31, 1996, Kluwer Acad. Publ, in press.